NeuroImage: Clinical 31 (2021) 102729

Contents lists available at ScienceDirect

NeuroImage: Clinical

journal homepage: www.elsevier.com/locate/ynicl

Altered cingulate structures and the associations with social awareness deficits and CNTNAP2 gene in autism spectrum disorder

Yi-Ling Chien [a], Yu-Chieh Chen [a,b], Susan Shur-Fen Gau [a,b,c,*]

[a] Department of Psychiatry, National Taiwan University Hospital and College of Medicine, Taipei, Taiwan
[b] Graduate Institute of Clinical Medicine, College of Medicine, National Taiwan University, Taipei, Taiwan
[c] Graduate Institute of Brain and Mind Sciences, College of Medicine, National Taiwan University, Taipei, Taiwan

ARTICLE INFO

Keywords:
Autism
Cingulate
Structure
Cortical thickness
CNTNAP2

ABSTRACT

Backgrounds: Although evidence suggests that the activity of the anterior cingulate cortex involves social cognition, there are inconsistent findings regarding the aberrant cingulate gray matter (GM) and scanty evidence about altered cortical thickness and white matter (WM) of cingulate in individuals with autism spectrum disorder (ASD). Evidence supports the association between the genetic variants of *CNTNAP2* and altered brain connectivity. This study investigated the cingulate substructure and its association with social awareness deficits and the *CNTNAP2* variants in individuals with ASD and typically-developing controls (TDC).

Methods: We assessed 118 individuals with ASD and 122 TDC with MRI and clinical evaluation. The GM, WM volumes and cortical thickness of the cingulate gyrus were compared between ASD and TDC based on fine parcellation. Five SNPs of the *CNTNAP2* linked to ASD and brain structural abnormality were genotyped, and rs2710102, rs2538991, rs2710126 passed quality control filters.

Results: ASD individuals showed thinner cortical thickness in bilateral cingulate subregions than TDC without significant group differences in GM and WM volumes. The WM volume of the right anterior cingulate gyrus was correlated with social awareness deficits in ASD. The *CNTNAP2* variant demonstrated a main effect on the WM volumes of the right middle cingulate gyrus. Besides, the *CNTNAP2* variants interacted with ASD diagnosis and age on the cortical thickness of the left anterior middle cingulate cortex.

Conclusions: Our findings suggest that aberrant cingulate structure in ASD might be associated with the social awareness deficits and genetic variants of the *CNTNAP2*. These novel findings need validation.

1. Introduction

Alterations of the cingulate structure are frequently reported in individuals with autism spectrum disorder (ASD) (Cauda et al., 2011). A meta-analysis of voxel-based morphometry (VBM) studies suggested that individuals with ASD (age range, 7 ~ 47 years old) showed a significant increase of grey matter (GM) volume in the subgenual anterior cingulate cortex (ACC) (Cauda et al., 2011). However, such associations were not supported by the other two meta-analyses (mean age, 8.9–38 years) (Nickl-Jockschat et al., 2012; Via et al., 2011). A recent meta-analysis focused on adults with ASD (mean age, 26 ~ 37.9 years; mean IQ, 97.4–123.6), instead reported reduced GM volume in the ACC (Yang et al., 2016). These inconsistent findings in ACC may be partially attributable to different age distribution and data acquisition across studies from multiple research sites. Beyond VBM studies, several existing reports only involved ACC but ignored other parts of the cingulate structure. Given that the cingulate cortex is anatomically and functionally heterogeneous and consists of distinct cytoarchitectonic zones that differ in cellular structures indicative of functional subdivision (Palomero-Gallagher et al., 2008; Simms et al., 2009), whether the subregions of the cingulate structure are altered in ASD in different patterns is worth investigation. Other than GM volume, ASD participants (aged 2–64) showed the increased cortical thickness of the posterior cingulate cortex (PCC) compared to typically-developing controls (TDC) in a meta-analysis of brain morphometry across ages (Cohen's $d = 0.13$) (van Rooij et al., 2018). Still, there was no significant difference in rostral and caudal ACC (van Rooij et al., 2018). In high-functioning adults with ASD (aged 18–62), however, cortical thickness of the right

* Corresponding author at: Department of Psychiatry, National Taiwan University Hospital and College of Medicine, No.7, Chung-Shan South Road, Taipei 10002, Taiwan.
E-mail address: gaushufe@ntu.edu.tw (S.S.-F. Gau).

https://doi.org/10.1016/j.nicl.2021.102729
Received 25 January 2021; Received in revised form 11 June 2021; Accepted 12 June 2021
Available online 19 June 2021

caudal ACC was significantly thinner than those of TDC (Laidi et al., 2019). Also, ASD was significantly associated with alterations of cortical thickness asymmetry in the cingulate area (Postema et al., 2019). As for white matter (WM) integrity, higher fractional anisotropy has been observed in the posterior cingulum of ASD toddlers (Xiao et al., 2014); whereas, lower-than-normal WM volumes along the cingulate arch has also been reported in ASD adults (Mitelman et al., 2017). Using probabilistic tractography to investigate deep intra-cingulate bundle (cingulum proper) and short cingulate U-fibers in 61 ASD youths and 54 TDC, increased mean and radial diffusivity of the left cingulum proper was observed in the ASD group (Hau et al., 2019), possibly indicating dysmyelination, demyelination (Alexander et al., 2007), or reduced axon packing density (defined as a total number within a sampling area) (Zikopoulos and Barbas, 2010; Zikopoulos et al., 2018). Compared to GM volume, the WM volume and cortical thickness of cingulate substructures remained controversial in ASD. A comprehensive assessment of cingulate substructures, including GM volume, WM volume, and cortical thickness, was lacking in ASD.

Regarding the function of the cingulate cortex, the ACC has been implicated in a broad range of behaviors and cognitive processes, including social cognition (Apps et al., 2016; Caruana et al., 2016; Patriquin et al., 2016). Using functional MRI to assess brain activation when doing the oddball social task, dorsal ACC activation was found to predict the severity of social impairments in a subset of ASD individuals (Dichter et al., 2009). By contrast, whether the structure of the cingulate cortex can predict social cognitive impairment in individuals with ASD is largely unknown. A study showing an association between increased thickness in the rostral ACC with more severe social impairment assessed by the Autism Diagnostic Interview-Revised (ADI-R) suggests that the cortical thickness of ACC may be correlated with the severity of social deficits in the individuals with ASD (Doyle-Thomas et al., 2013). Although evidence has implied the role of ACC in regulating social behaviors (Apps et al., 2016), it is unclear whether the other subregions of the cingulate also involve similar functions. In addition, new evidence supports that the middle cingulate cortex (MCC), previously noted as the dorsal ACC, may specifically affect social cognition (Apps et al., 2013). In contrast, the PCC may involve attention and arousal state (Leech and Sharp, 2014). Reduced functional coupling between PCC and ventromedial prefrontal cortex was highlighted in a recent meta-analysis that provided an early insight into the multiple dimensions of function, including higher-order cognitive function and complex social function (Lau et al., 2020). Given that MCC and PCC have been implicated in ASD-associated impairment such as social cognition (Apps et al., 2013) and attention (Leech and Sharp, 2014), whether these structural alterations are associated with social awareness deficits is of particular interest.

Recent studies have shown that brain structures such as total brain volume (Posthuma et al., 2000), cortical thickness (Jha et al., 2018; Schmitt et al., 2008; Thompson et al., 2001), and measures of white matter (WM) integrity derived from diffusion tensor imaging (Pfefferbaum et al., 2001) are all under moderate genetic control. Evidence suggests that several genes may play a role in regulating brain development. The contactin-associated protein-like 2 (CNTNAP2) gene encodes CASPR2, which is a member of the neurexin superfamily of transmembrane proteins that are responsible for voltage-gated K^+ channel clustering in juxtaparanodes (Poliak et al., 1999, 2003) at the nodes of Ranvier (Strauss et al., 2006). As a cell adhesion molecule responsible for neuroblast migration and laminar organization (Arking et al., 2008; Bakkaloglu et al., 2008; Vernes et al., 2008), CASPR2 is suggested to play a role in brain development. In cortical neuron cultures from mouse embryos, CASPR2 was lately demonstrated to play a dose-dependent role in axon growth *in vitro* (Canali et al., 2018). A study of an Amish family reported that a single-base deletion (3709delG) in the *CNTNAP2* gene might lead to a frameshift mutation. It manifested with seizures, language difficulties, and social deficits (Strauss et al., 2006). The homozygous mutations in exon 22 of the CNTNAP2 not only caused cortical dysplasia–focal epilepsy syndrome but also associated with neuropsychiatric outcomes, including intellectual disability (100% of cases), attention-deficit hyperactivity disorder (83%), and ASD diagnosis (67%) (Strauss et al., 2006), while polymorphism of rs2710102 (CC) and rs7794745 (TT) were associated with altered brain structure and functional connectivity in otherwise neurotypical subjects (Dennis et al., 2011; Scott-Van Zeeland et al., 2010; Whalley et al., 2011). On the other hand, mouse models lacking Cntnap2 gene presented with autistic behaviors, including repetitive behaviors and impairments in social interactions and communication (Peñagarikano et al., 2011, 2015; Scott et al., 2020). Loss of the *CNTNAP2* allele may contribute to abnormal neuronal migration (Reiner et al., 2016), decreased numbers of interneurons, and reduced cortical synchrony among the neuropathological abnormalities (Peñagarikano et al., 2011). These findings shed light on the functional consequences of CNTNAP2 disruption at the level of cortical structure. However, the effect of these rare deleterious variants in both *CNTNAP2* alleles in the brain does not also imply a role for *CNTNAP2* common variants in clinical phenotypes. Whether the common variants of *CNTNAP2* exert similar effects on the brain (or, more specifically, the neurons) waits to be elucidated.

Noteworthy, although the *CNTNAP2* has been proposed as an autism susceptibility gene (Alarcón et al., 2008; Anney et al., 2012; Arking et al., 2008; Bakkaloglu et al., 2008; Li et al., 2010; O'Roak et al., 2011), latest findings of genetic associations between the *CNTNAP2* and ASD in case-control studies were not replicated in recent larger ASD cohorts, including a replication study (Toma et al., 2013), large case-control cohorts of the Psychiatric Genomics Consortium (Toma et al., 2018), a family-based association study (on rs2710102 and rs7794745, etc.) (Zhang et al., 2019), and a screening study on rare heterozygous point mutations (Murdoch et al., 2015; Toma et al., 2018). Toma et al. (2018) concluded that although the genetic link between *CNTNAP2* variants and psychiatric phenotypes is tenuous, this does not dispel the evidence that the *CNTNAP2* variations may still have a real impact on neuronal functions or variability of brain connectivity.

The CNTNAP2 was reported to be associated with GM and WM volume (Tan et al., 2010; Uddén et al., 2017; Zhu et al., 2017) and structural disconnectivity (Clemm von Hohenberg et al., 2013; Dennis et al., 2011; Scott-Van Zeeland et al., 2010) in several regions that have already been implicated in ASD, including the cerebellum (Tan et al., 2010), fusiform gyrus, occipital (Uddén et al., 2017) and frontal cortices (Scott-Van Zeeland et al., 2010; Zhu et al., 2017). Several common variants of the *CNTNAP2* were reported to be associated with reduced GM volumes [e.g., rs7794745] (Tan et al., 2010; Uddén et al., 2017), structural connectivity [e.g., rs2710102 (Scott-Van Zeeland et al., 2010), rs2710126, rs759178, and rs2538991 (Clemm von Hohenberg et al., 2013)], and functional connectivity of the posterior right temporoparietal junction, a key node of the social network [e.g., rs2710102] (Bai et al., 2019). These variants overlap with the SNPs that were associated with early communicative difficulty (Alarcón et al., 2008; Newbury et al., 2011; Peter et al., 2011; Whitehouse et al., 2011) or social performance (Bai et al., 2019) in individuals with ASD, language disorder, or typically developing individuals, particularly the SNPs in intron 13 (Rodenas-Cuadrado et al., 2014). Both early communication difficulty and social deficits were hallmarks for the autism spectrum condition (American Psychiatric Association, 2013). The genetic effects of these five SNPs of the *CNTNAP2* gene would be tested herein to associate with the cingulate structures.

The current study aimed to investigate the cingulate structures in individuals with ASD and TDC. With a more delicate method of parcellation (Fig. 1), the subregions of cingulate GM (i.e., ACC, anterior MCC, posterior MCC, ventral and dorsal PCC), WM volumes (rostral ACC, caudal ACC, PCC, and isthmus), and cortical thickness (i.e., ACC, anterior MCC, posterior MCC, ventral and dorsal PCC) were analyzed. We examined whether age, sex, and autistic symptoms were significant correlates of cingulate structures. Besides, we investigated the genetic associations between the cingulate structures and the *CNTNAP2* variants

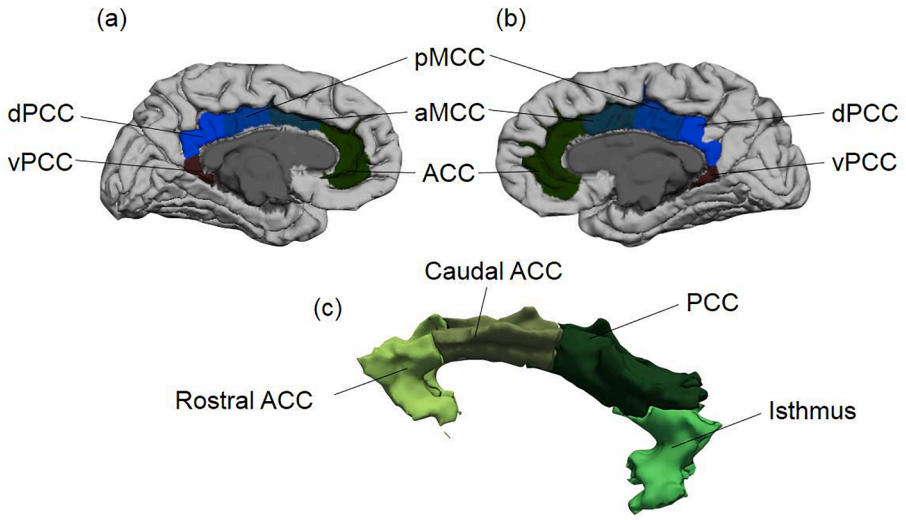

Fig. 1. Cingulate substructures on FreeSurfer. (a) the left cingulate gyrus, (b) the right cingulate gyrus, (c) the cingulate substructures. [Abbreviations. ACC: anterior cingulate cortex; PCC: posterior cingulate cortex; aMCC: anterior part of middle cingulate cortex; pMCC: posterior part of middle cingulate cortex; dPCC: dorsal part of posterior cingulate cortex; vPCC: ventral part of posterior cingulate cortex]

(i.e., rs7794745, rs759178, rs2710102, rs2538991, and rs2710126) that were repetitively shown to be associated with brain structure or connectivity. We hypothesized that individuals with ASD might have abnormal cingulate structures compared to TDC, and these structural alterations were possibly related to the severity of social awareness deficits. We also hypothesized that *CNTNAP2* variants might play a role in modifying the cingulate substructures of ASD.

2. Materials and Methods

2.1. Participants

We collected brain MRI scans, clinical and genetic data from a total sample of 118 individuals with ASD (mean 13.1 years, SD 4.6; male 113, 95.8%), and 122 TDC (mean 21.0, SD 9.7; male 75, 61.5%). Individuals with ASD were recruited from National Taiwan University Hospital, Taipei, Taiwan. They were clinically diagnosed as ASD by senior board-certified child psychiatrists based on the Diagnostic and Statistical Manual of Mental Disorders-5th edition (DSM-5) diagnostic criteria of autism spectrum disorder; the diagnosis was further confirmed by a structural interview using the Chinese version of the ADI-R (Gau et al., 2011; Lord et al., 1994). Participants with major neuropsychiatric disorders or a full-scale IQ lower than 70 were excluded (n = 2, full-scale IQs 67 and 68). The TDC participants were recruited from schools in the same districts as the ASD participants and advertisements. All the participants were ethnic Han Chinese. Detailed family history was collected to ensure that every first- or second-degree relative was Han Chinese and that no first- or second-degree relatives of TDC had a diagnosis of ASD. All the participants went on clinical evaluation and interviews; all their parents were also interviewed by using the Chinese version of the Kiddie epidemiologic version of the Schedule for Affective Disorders (K-SADS-E) interview (Chen et al., 2017; Gau et al., 2005) to exclude any current or lifetime ASD and other major psychiatric disorders including attention-deficit hyperactivity disorder, schizophrenia, mood disorders, anxiety disorders, or neurodevelopmental disorders. The psychometric properties of the Chinese version of the K-SADS-E and interview training have been described elsewhere (Chen et al., 2017, 2019; Gau et al., 2005, 2010).

2.2. Procedure

The Research Ethics Committee approved the study before its implementation (Approval number: 201201006RIB; ClinicalTrials.gov number, NCT01582256). After the purposes and procedures of the study were fully explained and confidentiality was assured, written informed consent was obtained from the participants and their parents. All the participants were then assessed with the brain MRI and the *Wechsler Intelligence Scale for Children (version III)* or the *Wechsler Adult Intelligence Scale (version IV)* for the IQ profiles according to their ages. The parents (mainly mothers) completed the following clinical measures about the participants.

2.3. Measures

The *ADI-R* (Lord et al., 1994) is a standardized, comprehensive, semi-structured, investigator-based interview for the caregivers of children with a mental age of 18 months into adulthood. It covers most developmental and behavioral aspects of ASD, including qualitative abnormalities in reciprocal social interaction, communication, and restricted, repetitive and stereotyped patterns of behaviors. The Chinese version of the ADI-R was approved by the Western Psychological Services in 2007 and has been widely used in several studies to validate the clinical diagnosis of ASD, e.g., (Chien et al., 2017; Ni et al., 2018; Yin et al., 2016). The details of psychometric studies and interviewers' training of using the Chinese ADI-R have been described elsewhere (Chiang et al., 2018; Gau et al., 2013).

The *Social Responsiveness Scale (SRS)* (Constantino and Gruber, 2005) is a widely-used quantitative measure of autistic traits in the general population. It includes 65 items to measure the severity of ASD symptoms in natural social settings over the past six months for children and adolescents aged 4–18. Items were rated by parents or caregivers on a 4-point Likert scale from "0" (not true) to "3" (almost always true). The SRS has been demonstrated to have good internal consistency, construct validity, inter-rater reliability, test–retest reliability, and discriminative validity in prior research (Constantino and Gruber, 2005). Its Chinese version demonstrates a four-factor structure (i.e., social communication, stereotyped behaviors/interest, social awareness, and social emotion). Still, it is better conceptualized as a one-factor model (Gau et al., 2013). The Chinese SRS has been widely used in ASD research from children to young adults in Taiwan, e.g., (Chen et al., 2017; Hsiao et al., 2013; Lau et al., 2014; Lo et al., 2019), that covered the age range of our ASD sample. High internal consistency was found for the four subscales (Cronbach's alpha, 0.94–0.95) and the total scale (Cronbach's alpha, 0.95). To test the association between cingulate structures and social

cognition, we specifically targeted the social awareness deficits subscale in this study. This subscale is composed of 11 items of the SRS, including items 3, 7, 12, 15, 17, 21, 26, 32, 38, 45, and 52 (Gau et al., 2013). These items rated the level that the subject can be aware of what others feel or think, the level that the subject can respond to the mood changes in others, etc. We summed up the 11 item responses after the reversed items were rescored.

2.4. Single nucleotide polymorphism (SNP) selection and genotyping

Genomic DNA was prepared from peripheral blood using the Puregene DNA purification system (Gentra Systems Inc. Minneapolis, MI) according to the manufacturer's instructions. Five SNPs of the *CNTNAP2*, located in the intron 2 (rs7794745) (Tan et al., 2010; Uddén et al., 2017), intron 13 (rs759178, rs2710102, rs2538991) (Bai et al., 2019; Clemm von Hohenberg et al., 2013; Scott-Van Zeeland et al., 2010), and intron 15 (rs2710126) (Clemm von Hohenberg et al., 2013), were selected for genotyping based on previous imaging genetic studies.

The primers of each SNP were designed by the platform of the National Center for Genome Medicine (http://ncgm.sinica.edu.tw/), using GenePipe (http://genepipe.ncgm.sinica.edu.tw/seqtool/pages/getSeq.jsp) to retrieve SNP flanking sequences. All SNP genotyping was performed by SEQUENOM MassARRAY® System using matrix-assisted laser desorption/ionization-time of flight mass spectrometry. The genotyping technology platform "iPLEX ® Gold reaction" provides high throughput, high accuracy, and low-cost SNP analysis (http://ncgm.sinica.edu.tw/ncgm_02/snp_platform_e.html). The success rate of genotyping of the five selected SNPs were 99–100%. All SNPs were not against the Hardy-Weinberg equilibrium (Supplementary Table S1). The SNP rs7794745 was excluded, given its minor allele frequency significantly deviated from the dataset on the public domain (dbSNP). The SNP rs759178 was also removed, given its high linkage disequilibrium with rs2538991 ($r^2 > 0.97$) and similar genotype frequency between the two SNPs. Genotype frequency is summarized in Supplementary Table S2. The age distribution was not different across genotypes ($p > 0.236$) (Supplementary Table S3).

2.5. MRI data acquisition

Brain images were acquired on a 3 T MRI system (Trio, Siemens, Erlangen, Germany). Head movement was restricted with expandable foam cushions and was assessed immediately after image acquisition. High-resolution T1-weighted images were obtained on a 3 T MRI scanner (Siemens Magnetom Tim Trio, Germany) using a 32-channel phased arrayed head coil and a 3D magnetization prepared rapid acquisition gradient echo (MPRAGE) (Repetition/echo time = 2,000/2.98 ms; inversion time = 900 ms; flip angle = 9°; matrix size = 256 × 256 × 192; voxel size = 1 mm^3).

2.6. Whole brain segmentation and cortical thickness calculation.

FreeSurfer V5.2.0 (https://surfer.nmr.mgh.harvard.edu/) was used on a 64-bit Linux operating system to reconstruct the cortical surface and volumetric segmentation on each participant's T1 image based on the MPRAGE images (Fischl, 2012). The processing pipeline we implemented included the removal of non-brain tissue (Ségonne et al., 2004), automated Talairach transformation, segmentation of subcortical white matter and deep GM volumetric structures (Fischl et al., 2004a), intensity normalization (Sled et al., 1998), tessellation of GM and WM boundaries, automated topology correction (Segonne et al., 2007), and surface deformation for optimal placement of GM/WM and GM/cerebrospinal fluid borders (Dale et al., 1999). The borders (i.e., GM vs. WM, GM vs. cerebrospinal fluid) were manually corrected to match anatomical boundaries based on careful visual inspection. Specifically, the pial surface and WM surface were edited to correct their surface boundary to remove non-brain tissue and incorrect segmentation of GM and WM tissue. To enhance intensity normalization, we set control points at the areas with extreme intensity, which may interfere WM segmentation and lead to errors in the WM surface boundary. Lastly, we ensured that each participant had the Euler number (a measure of the topological complexity of the reconstructed cortical surface as calculated by the sum of the vertices and faces subtracted by the number of faces (Dale et al., 1999)) precisely at 2 for each hemisphere, indicating adequate data quality (Rosen et al., 2018). All participants (n = 240) were realigned to the study-specific template using the Freesurfer registration template to create the age-specific surface and curvature for each participant. Whole brain segmentation (Fischl et al., 2002, 2004b) was performed with default parameters of the FreeSurfer. The cortical parcellation units of the cortex were automatically identified and labeled according to the Desikan atlas (Desikan et al., 2006) within the FreeSurfer automatic cortical parcellation routine. The cortical thickness was automatically calculated by computing the shortest distance between the WM boundary and the pial surface at each vertex (Fischl and Dale, 2000). The reliability of the cortical thickness calculated by FreeSurfer has been validated (Han et al., 2006). The automatic reconstruction and calculation were reprocessed after manually correcting the detected erroneous part. The automatic parcellation of cortical regions derived 74 brain regions in each hemisphere, and the thickness of each cortical region was then calculated. This study focused on the cingulate substructures, in which GM was divided into five subregions, i.e., ACC, anterior and posterior parts of MCC, and dorsal and ventral parts of PCC, while WM was divided into four subregions, i.e., the rostral ACC, caudal ACC, PCC, and isthmus (Fig. 1).

2.7. Statistical analysis

We used SAS 9.4 (SAS Institute Inc, Cary NC, USA) to perform the statistical analyses. Age and IQ profiles were compared by analysis of variance, while SRS subscores were compared between the ASD and TDC groups by the general linear model controlling for sex and age. Because the ASD participants were younger than TDC in the whole sample (age range 6–52), we compared the volume of the GM and WM, and cortical thickness of cingulate structures for each subregion between ASD and TDC in an age- and sex-matched subsample (88 ASD & 51 TDC, aged 8–20), controlling for sex, age, full-scale IQ, handedness, and intracranial volume. The relationships between the cingulate structures and social awareness deficits were examined by Pearson's correlation analyses in the ASD group, partial out the effects of age, sex, full-scale IQ, and intracranial volume. The genetic effects of the *CNTNAP2* variants on the cingulate structures were firstly examined by the main effect of each SNP on cingulate substructures (i.e., GM and WM volumes, and cortical thickness of each subregion) [Model 1: Cingulate structure parameters $= \beta_0 + \beta_1$ SNP $+ \beta_2$ Diagnosis $+ \beta_3$ Sex $+ \beta_4$ Age $+ \beta_5$ Intracranial volume $+ \varepsilon$]. Then, we tested the interactions between the *CNTNAP2* variants and age or diagnosis on each cingulate structure, controlling for age, sex, full-scale IQ, and intracranial volume, as well as the main effects of each SNP and diagnosis [Model 2: Cingulate structure parameters $= \beta_0 + \beta_1$ SNP $+ \beta_2$ Diagnosis $+ \beta_3$ Sex $+ \beta_4$ Age $+ \beta_5$ (SNP × Group) $+ \beta_6$ (SNP × Age) $+ \beta_7$ (SNP × Group × Age) $+ \beta_8$ Intracranial volume $+ \varepsilon$]. False discovery rate (FDR) was applied to correct for multiple comparisons. FDR q-value < 0.05 was set as statistical significance. As for sensitivity power analysis, with a total sample size of 240, the statistical tests had a power of 0.8 to detect a difference with the effect size of 0.27.

3. Results

The IQ profiles of the whole sample were within the normal range, while the ASD group had significantly lower full-scale IQ (100.8 ± 19.9) compared to the TDC (116 ± 10.9) (Table 1). The ADI-R subscores of the ASD group passed the cut-off of a diagnosis of autism at the most severe period (age of 4–5 years): Social Reciprocal Interaction, 19.68 ± 6.98; Verbal Communication, 14.69 ± 5.03; Non-verbal Communication,

Table 1
Demographic data and autistic symptoms measured on the Social Responsiveness Scale and Autism Diagnostic Interview-Revised.

	ASD (N = 118)		TDC (N = 122)		F	p
	Mean or N	SD or (%)	Mean or N	SD or (%)		
Age	13.1	4.6	20.9	9.7	63.27	<0.0001
Male (%)	N = 113	(95.8)	N = 75	(61.5)	41.55	<0.0001
Handedness						
Verbal IQ	100.8	19.9	111.6	10.9	28.51	<0.0001
Performance IQ	99.7	21.1	111.5	13.3	26.99	<0.0001
Full-scale IQ	100.1	20.1	112.3	11.7	33.31	<0.0001
Autism Diagnostic Interview-Revised						
Most severe at 4–5 years						
Social reciprocal interaction	19.68	6.98	–	–	–	–
Communication: Verbal	14.68	5.03	–	–	–	–
Nonverbal	7.84	3.43	–	–	–	–
Repetitive/ stereotyped behavior/ interests	7.26	2.67	–	–	–	–
Current						
Social reciprocal interaction	10.29	4.71	–	–	–	–
Repetitive/ stereotyped behavior/ interests	5.27	2.52	–	–	–	–
Social Responsiveness Scale						
Social awareness deficits	20.57	5.29	12.50	5.95	78.05	<0.0001

7.84 ± 3.43; Repetitive/Stereotyped Behavior/Interests, 7.26 ± 2.67 (Table 1). The social awareness deficits measured by the SRS were significantly more severe in the ASD group compared to the TDC group (Table 1).

3.1. Group comparison in cingulate structures

In the age- and sex-matched subsample, there were no significant group differences in GM and WM volumes of each cingulate subregion except a larger WM volume in the isthmus part of the cingulate in individuals with ASD than TDC (Table 2). By contrast, ASD participants had thinner cortical thickness than TDC in the following subregions: the right ACC, right anterior MCC, bilateral posterior MCC, and bilateral ventral and dorsal PCC (Table 2). The most significant difference was found in the right posterior MCC thickness (Cohen's $d = -0.578$). The significant differences between ASD and TDC generally remained in the whole sample (Supplementary Table S4). In addition, cingulate substructures were not significantly different between adolescents (n = 58) and children (n = 49) with ASD after controlling age, sex, full-scale IQ, and intracranial volumes (Supplementary Table S5). Therefore, we did not conduct correlation analysis stratifying by the child and adolescent groups.

3.2. Correlations between cingulate structures and autistic symptoms in ASD

Correlation analyses between cingulate structures and social awareness deficits revealed a significant negative correlation between the WM volume of the right caudal ACC and social awareness deficits on SRS ($r = -0.313$, p = 0.001) (Fig. 2). There were no significant correlations between social awareness and GM volumes or cortical thickness.

3.3. CNTNAP2 genetic association with cingulate structures

The SNP rs2538991 was significantly associated with the WM volume of the right caudal anterior cingulate gyrus [GG (n = 79) 3188.7 ± 528.4, GT (n = 127) 2950.5 ± 422.1, TT (n = 31) 3197.3 ± 559.4 ($F_{(4,232)} = 6.75$, p = 0.0014); post-hoc analysis, GG, TT > GT, Bonferroni correction $p < 0.05$] (Fig. 3). However, the heterozygotes (GT), but not the homozygous carriers (GG), showed the smallest WM volume.

We further conducted multiple regression analyses for each SNP model, including the main effect of each SNP, two-way interactions (SNP × age, SNP × diagnosis), and three-way interaction (SNP × age × diagnosis). For the model containing both two-way interactions and three-way interaction, the same SNP rs2538991 (Supplementary Fig. S1a), and rs2710102 (Supplementary Fig. S1b) interacted with age and diagnosis group on the cortical thickness of the same region, i.e., the left anterior MCC (Supplementary Table S6). We tested the above results using the allelic model for analysis. However, findings in genotype analysis were not significant in the allelic analysis ($p > 0.47$) (Supplementary Table S7). Given that none of ASD participants were older than 33 years, we conducted the same analyses shown above by removing TDC participants older than 33 years (n = 13) and found that the significant results remained (Supplementary Table S8).

4. Discussion

Our work is one of the first studies to report the altered cingulate substructures with delicate parcellation in individuals with ASD, including GM and WM volumes and cortical thickness. It is also the first to explore the relationships between cingulate substructures and the *CNTNAP2* gene. The major findings are three folds. First, individuals with ASD showed the thinner cortical thickness of bilateral cingulate subregions, greater WM volume of the isthmus, and no difference in the cingulate GM volume. Second, decreasing WM volumes of the right caudal anterior cingulate gyrus was associated with increasing social awareness deficits. Third, the *CNTNAP2* variant was associated with the WM volumes of the right caudal anterior cingulate gyrus and interacted with ASD diagnosis on the cortical thickness of the left anterior MCC only in genotype analysis rather than allelic model analysis.

Our finding that ASD youths showed a greater WM volume of isthmus than TDC has not been reported. Previous studies have demonstrated greater left cingulum proper without differences in rostral anterior, caudal anterior, posterior, and isthmus cingulate U-fibers in ASD youths (Hau et al., 2019), or smaller WM volumes along the cingulate arch in ASD adults (Mitelman et al., 2017). Given the cingulate body connected to the parahippocampal gyrus via the isthmus, whether the greater WM volume of the isthmus here reflects impaired limbic connectivity like previously suggested (Ameis and Catani, 2015) needs further investigation. Meanwhile, although we found no significant difference in cingulate GM volumes, which was consistent with some previous studies (Nickl-Jockschat et al., 2012; Via et al., 2011), our results demonstrated that the cortical thickness of most subregions was significantly thinner in ASD compared to TDC. Our finding was consistent with a recent study in ASD adults, showing thinner caudal ACC thickness in both the discovery (n = 301) and the replication sample (n = 61) (Laidi et al., 2019), yet contradictory to previous studies showing either no difference in rostral and caudal ACC thickness (van Rooij et al., 2018), or increased cortical thickness of the left cingulate (in 19 adults with high-functioning autism (Libero et al., 2015)), bilateral PCC (in 15 young adult males with autism (Hyde et al., 2010) and a meta-analysis (van Rooij et al., 2018)), and the left MCC (in 22 children with ASD aged 9.2 ± 2.1 years (Jiao et al., 2010)). Our results were based on a comparison between 88 ASD and 51 TDC with careful adjustment on sex, age, full-scale IQ, handedness, and intracranial volume. Consistent with a previous finding on significant age by group interaction across the cingulate substructures (van Rooij et al., 2018), our finding showed that age was a significant covariate for cortical thickness in most cingulate

Table 2
Group comparison of cingulate structures.

	ASD (N = 88)		TDC (N = 51)				
	Mean or N	SD or (%)	Mean or N	SD or (%)	F	P	
Age (age range)	12.7 (8–20)	3.1	13.8 (8–20)	3.6	3.24	0.074	
Male	N = 84	(95.5)	N = 45	(88.2)	2.52	0.112	
Left-handedness	N = 80	(98.9)	N = 48	(94.1)	0.46	0.499	
Full-scale IQ	104	15.6	113	12.5	13.51	0.0003	
Mean thickness (mm)							
R. hemisphere	3.101	0.169	3.157	0.100	7.47	0.007	
L. hemisphere	3.108	0.165	3.158	0.107	6.73	0.011	
White matter volumes (mm^3)							**Cohen's *d***
R. caudal anterior cingulum	3092	431	3124	513	0.02	0.891	–
R. isthmus of cingulum	3488	500	3358	400	9.97	0.002*	0.287
R. rostral anterior cingulum	2155	303	2215	339	0.73	0.395	–
R. posterior cingulum	4466	565	4456	489	0.41	0.524	–
L. caudal anterior cingulum	2933	472	2949	483	0.04	0.849	–
L. isthmus of cingulum	3871	600	3689	457	8.79	0.004*	0.341
L. rostral anterior cingulum	2697	392	2670	364	1.48	0.227	–
L. posterior cingulum	4454	542	4323	501	2.02	0.157	–
Cortical thickness (mm)							**Cohen's *d***
R. ACC	3.45	0.27	3.55	0.21	6.93	0.010*	−0.426
R. anterior MCC	3.52	0.23	3.58	0.22	5.53	0.020*	−0.264
R. posterior MCC	3.38	0.22	3.50	0.17	14.46	0.000*	−0.578
R. dorsal PCC	3.71	0.24	3.81	0.20	6.79	0.010*	−0.442
R. ventral PCC	3.38	0.37	3.52	0.31	5.54	0.020*	−0.410
L. ACC	3.50	0.26	3.55	0.19	2.59	0.110	–
L. anterior MCC	3.49	0.26	3.56	0.20	3.88	0.051	–
L. posterior MCC	3.37	0.24	3.46	0.18	8.70	0.004*	−0.396
L. dorsal PCC	3.72	0.27	3.82	0.19	6.57	0.012*	−0.398
L. ventral PCC	2.90	0.41	3.06	0.37	5.50	0.021*	−0.404
Cortical volume (mm^3)							
R. ACC	6983	934	6803	814	1.48	0.226	–
R. anterior MCC	3837	586	3880	492	0.09	0.770	–
R. posterior MCC	3696	527	3679	584	0.03	0.870	–
R. dorsal PCC	1957	399	1888	335	2.72	0.102	–
R. ventral PCC	870	218	949	222	2.56	0.112	–
L. ACC	6029	951	5899	649	0.68	0.411	–
L. anterior MCC	3478	551	3519	600	0.35	0.554	–
L. posterior MCC	3259	407	3256	422	0.01	0.909	–
L. dorsal PCC	2063	470	1995	373	0.31	0.577	–
L. ventral PCC	865	220	879	224	0.01	0.936	–

Note. *False Discovery Rate q-value < 0.05; L, left; R, right; ACC, anterior cingulate cortex; MCC, middle cingulate cortex; PCC, posterior cingulate cortex
Cohen's *d* values are presented for those with False Discovery Rate q-value < 0.05.

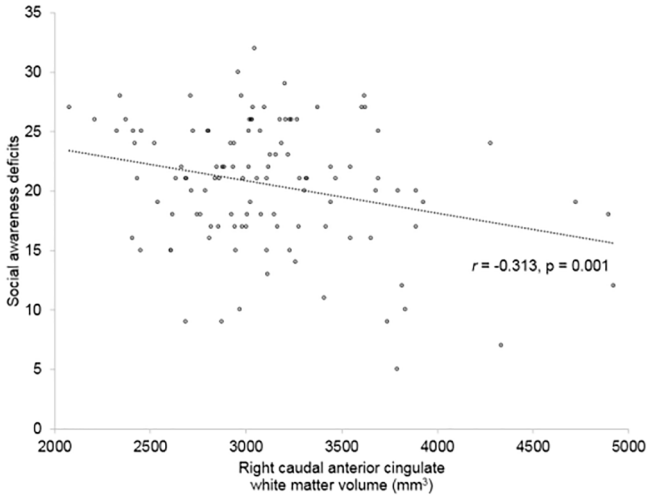

Fig. 2. Correlation between cingulate structure and social awareness deficits in individuals with autism spectrum disorder. The right anterior cingulate white matter volume was negatively correlated with social awareness deficits (r = -0.313, p = 0.001).

subregions in our study (except PCC), supporting a previous argument that ASD is characterized by complex alterations in lifetime trajectories of several brain regions that underpin social-cognitive function (Greimel et al., 2013). Whether the cortical thinning in the cingulate gyrus of ASD individuals was abnormal, specifically during adolescence, waits to be answered. In contrast to previous findings of reduced cingulate GM volume in adults with ASD (Toal et al., 2009; Yang et al., 2016), in our sample of youths aged 8–20, we did not find group differences in the cingulate GM volume. Whether different age groups of the study samples can explain the inconsistent findings warrants further investigation.

Our finding that the WM volumes of the caudal anterior cingulate gyrus (MCC) was negatively correlated with social awareness deficits worths research. Although the function of the cingulate gyrus has been implicated in social cognition, only a few studies investigated the relationship between cingulate structure and autistic symptoms. For cortical thickness, increased thickness in the rostral ACC has been associated with poorer Social subscores on the ADI-R (Doyle-Thomas et al., 2013); likewise, higher ADOS scores were associated with increased thickness in the cingulate cortex (van Rooij et al., 2018). Another study reported that social awareness deficits were correlated with increased functional connectivity between the dorsal ACC (namely MCC in this study) and right superior temporal gyrus and decreased functional connectivity between the dorsal ACC and right putamen and thalamus (Tu et al., 2016). As for the WM integrity of the cingulum, previous findings were

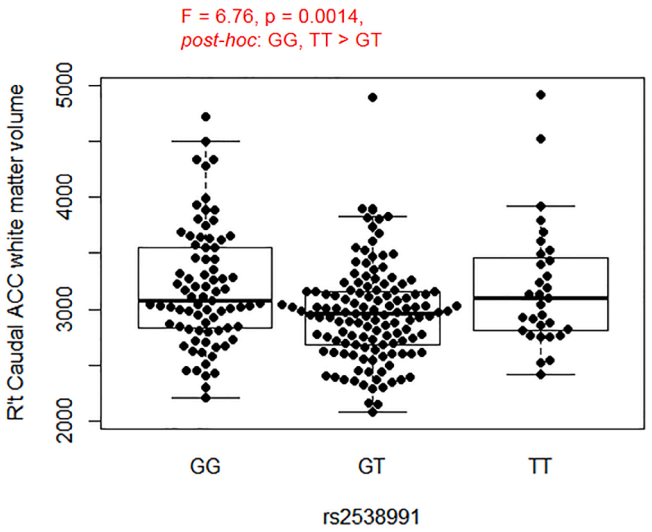

Fig. 3. Associations between CNTNAP2 variants and cingulate structure (a) rs759178 vs. right caudal anterior cingulate white matter volume: GG (n = 78) 3187.5 ± 531.7, GT (n = 127) 2951.3 ± 422.7, TT (n = 31) 3197.3 ± 559.4 (F = 6.76, p = 0.0014); post-hoc analysis, GG, TT > GT (b) rs2538991 vs. right caudal anterior cingulate white matter volume: GG (n = 79) 3188.7 ± 528.4, GT (n = 127) 2950.5 ± 422.1, TT (n = 31) 3197.3 ± 559.4 (F = 6.75, p = 0.0014); post-hoc analysis, GG, TT > GT (c) rs779475 vs. right ventral posterior cingulate cortical thickness: TA (n = 35), 3.49 ± 0.33; TT (n = 201), 3.34 ± 0.34; F = 7.13, p = 0.0081.

inconsistent. One reported no relationship between socio-communicative symptoms and cingulum micro- or macrostructural measures in adult males with ASD (Catani et al., 2016), yet, a negative relationship between fractional anisotropy of right cingulum (hippocampal part) and social awareness (on the SRS) has been reported in younger adults with ASD (Chiang et al., 2017). Using probabilistic tractography, a recent study demonstrated that the ADI-R Social subscore was positively correlated with the volume and negatively correlated with the left posterior cingulate U-fiber integrity. Taken together, our results that ASD youths had a thinner cingulate cortex and that smaller right MCC WM volume was correlated with more severe social awareness deficits indicate that the quantitative trait of social cognition may be associated with cingulate structural variations linked to ASD. These findings, if verified, implied a potential role of the cingulate gyrus in modulating the core symptoms of ASD.

As the first study to focus on the genetic association between the *CNTNAP2* variants and cingulate structures, we found that the *CNTNAP2* variant was associated with the right MCC WM volume (rs2538991) in genotype analysis (so did the rs759178; data not shown because its high linkage disequilibrium with rs2538991). Several studies support that *CNTNAP2* plays a role in regulating brain connectivity. Children carrying the autism risk allele (C) of rs2710102 showed reduced long-range functional connectivity (i.e., fronto-occipital connectivity) but increased short-range functional connectivity (Scott-Van Zeeland et al., 2010). Another study used whole-brain tractography and graph metrics to compare structural connectivity between genotypes of this SNP; the result also supported the association between this SNP and the reduced long-range brain connectivity (Dennis et al., 2011). A neighbor SNP, rs2710126, was also reported to associate with structural connectivity of the uncinate fasciculus (Clemm von Hohenberg et al., 2013). Several SNPs located in intron 13 (i.e., rs2710102, rs759178, and rs2538991) were found nominally associated with axial diffusivity of the dorsal cingulum bundle (Clemm von Hohenberg et al., 2013). Our findings did not support the association between rs2710102 and cingulate substructures but showed an association between the SNP rs2538991 and MCC WM volume in genotype analysis but not allelic model analysis. Notably, the GT genotype of rs2538991 had the smallest MCC WM volume. This might explain why the significant findings in genotype analysis disappeared in allelic analysis. Whether our finding implied a true association between CNTNAP2 and cingulate structure needs validation. A review article that collected *CNTNAP2* disruptions and associated phenotypes concluded that most disruptions of the *CNTNAP2* are heterozygous mutations, suggesting that loss of a single allele could be sufficient to cause a phenotype (Rodenas-Cuadrado et al., 2014). Such observation may not be the story in common variants. Nevertheless, evidence has shown that polymorphism of CNTNAP2 was associated with altered brain structure and functional connectivity in neurotypical subjects (Dennis et al., 2011; Scott-Van Zeeland et al., 2010; Whalley et al., 2011). The role of polymorphisms on SNP interaction or epistasis warrants further investigation.

Given the distinct developmental trajectories in the ASD brain, particularly the GM volume of the MCC (Greimel et al., 2013), we specifically tested whether the *CNTNAP2* variants interacted with age on the cortical thickness of two components of MCC, the anterior and posterior MCC, separately. We found a group × age × SNP interaction on the left anterior MCC only for the SNPs in intron 13 of the *CNTNAP2* (i.e., rs2538991 and rs2710102; same in rs759178 but data not shown due to high linkage disequilibrium between rs759178 and rs2538991), which might suggest the effect of intron 13 on cortical thinning differs between ASD and TDC. The finding that ASD carriers of TT genotype showed a faster cortical thinning with age than TDC counterparts with the same genotype (Supplementary Fig. S1) needs to be replicated in a larger sample with an adequate number of minor alleles. Also, as a cross-sectional study, the age effect can hardly be addressed by the developmental approach. A longitudinal study may further help to elucidate the effect of the allele on cortical thinning.

This study had several limitations. First, the ASD participants of the whole sample were male predominant and younger than controls. Hence, cingulate substructures were compared in a sex- and age-matched subsample and the findings in the matched subsample were generally consistent in the whole sample. A low female rate may also limit our findings' generalizability, which needs to be validated in a sample with a sex ratio closer to the canonical ratio of the ASD population. Second, we measured social awareness deficits by a caregiver-reported questionnaire rather than a social cognition task. Although the observation from caregivers may better reflect the social function of ASD participants in daily life (particularly for the ASD youth), a social cognition task that targets the specific social deficit of ASD (e.g., (Boada et al., 2020)) may provide a standard objective measure and thus should be considered. Third, although the number of our sample is one of the large-scale imaging genetic studies in ASD, the sample size of the current study still may not have adequate power to detect small effect differences in the scale of gene research, which is particularly true for common variants. A larger independent sample is needed to verify our results and may allow for further analysis stratified by age (e.g., childhood vs. adolescence). Fourth, the candidate SNPs selected in this study were based on previous imaging genetic studies of the *CNTNAP2*. Future studies may consider fine mapping or sequencing of this gene. Lastly, participants with full-scale IQ lower than 70 were excluded from the study considering the cooperativeness of the participants undergoing MRI procedures. The results may not be generalized to the individuals with lower IQ.

5. Conclusions

This study's findings suggest that youths with ASD showed comparable GM and WM volume but reduced cortical thickness of bilateral cingulate subregions compared to TDC. Besides, the cingulate structure may have clinical implications on moderating the severity of social awareness deficits, particularly the right cingulate WM volume. The brain-behavior relationships between cingulate substructures and the specific symptom domains may benefit from a delicate parcellation of the cingulate gyrus. Furthermore, as one of the first studies to explore

the relationship between *CNTNAP2* and altered cingulate structures, our preliminary findings in genotype analysis warrant larger independent samples to validate.

Declarations

Ethics approval and consent to participate

This work has been carried out in accordance with the Code of Ethics of the World Medical Association (Declaration of Helsinki) for experiments involving humans. The Research Ethics Committee approved the study before its implementation (Approval number: 201201006RIB).

Funding

This study was supported by grants from the Ministry of Science and Technology [grant numbers: NSC99-2321-B-002-037, NSC100-2321-B-002-015, NSC 101-2314-B-002-136-MY3, MOST102-2314-B-002-019-, MOST106-2410-H-002-075-MY2, MOST108-2628-H-002-009-MY3]; National Health Research Institute [NHRI-EX104-10404PI, NHRI-EX105-10404PI, NHRI-EX106-10404PI, NHRI-EX107-10404PI]; National Taiwan University Hospital [NTUH101-S1910, NTUH101-M2004, NTUH108-S4103]; and Chen-Yung Foundation, Taiwan.

CRediT authorship contribution statement

Yi-Ling Chien: Conceptualization, Formal analysis, Writing - original draft, Funding acquisition. **Yu-Chieh Chen:** Software, Data curation, Visualization, Formal analysis. **Susan Shur-Fen Gau:** Conceptualization, Methodology, Investigation, Supervision, Writing - review & editing, Project administration, Funding acquisition.

Declaration of Competing Interest

The authors declare that they have no known competing financial interests or personal relationships that could have appeared to influence the work reported in this paper.

Acknowledgments

We thank the National Center for Genome Medicine of the National Core Facility Program for Biotechnology, Ministry of Science and Technology, for the technical/bioinformatics support. We also thank the Department of Medical Imaging and the Eighth Core Lab, Department of Medical Research, National Taiwan University Hospital for MRI scans and technical support, respectively, during the study.

Appendix A. Supplementary data

Supplementary data to this article can be found online at https://doi.org/10.1016/j.nicl.2021.102729.

References

Alarcón, M., Abrahams, B.S., Stone, J.L., Duvall, J.A., Perederiy, J.V., Bomar, J.M., Sebat, J., Wigler, M., Martin, C.L., Ledbetter, D.H., Nelson, S.F., Cantor, R.M., Geschwind, D.H., 2008. Linkage, association, and gene-expression analyses identify CNTNAP2 as an autism-susceptibility gene. Am. J. Hum. Genet. 82 (1), 150–159.

Alexander, A.L., Lee, J.E., Lazar, M., Field, A.S., 2007. Diffusion tensor imaging of the brain. Neurotherapeutics 4 (3), 316–329.

Ameis, S.H., Catani, M., 2015. Altered white matter connectivity as a neural substrate for social impairment in Autism Spectrum Disorder. Cortex 62, 158–181.

American Psychiatric Association, 2013. Diagnostic and Statistical Manual of Mental Disorders, 5th ed. American Psychiatric Publishing, Arlington, VA.

Anney R, Klei L, Pinto D, Almeida J, Bacchelli E, Baird G, et al. Individual common variants exert weak effects on the risk for autism spectrum disorders. Hum. Mol. Genet. 2012;21:4781–4792.

Apps, M.A., Lockwood, P.L., Balsters, J.H., 2013. The role of the midcingulate cortex in monitoring others' decisions. Front. Neurosci. 7, 251.

Apps, M.J., Rushworth, M.S., Chang, S.C., 2016. The Anterior Cingulate Gyrus and Social Cognition: Tracking the Motivation of Others. Neuron 90 (4), 692–707.

Arking, D.E., Cutler, D.J., Brune, C.W., Teslovich, T.M., West, K., Ikeda, M., Rea, A., Guy, M., Lin, S., Cook, E.H., Chakravarti, A., 2008. A common genetic variant in the neurexin superfamily member CNTNAP2 increases familial risk of autism. Am. J. Hum. Genet. 82 (1), 160–164.

Bai T, Zhang L, Xie X, Xiao G, Huang W, Li D, et al. Common variant of CNTNAP2 gene modulate the social performances and functional connectivity of posterior right temporoparietal junction. Soc. Cogn. Affect Neurosci. 2019;14:1297-1305.

Bakkaloglu, B., O'Roak, B.J., Louvi, A., Gupta, A.R., Abelson, J.F., Morgan, T.M., Chawarska, K., Klin, A., Ercan-Sencicek, A.G., Stillman, A.A., Tanriover, G., Abrahams, B.S., Duvall, J.A., Robbins, E.M., Geschwind, D.H., Biederer, T., Gunel, M., Lifton, R.P., State, M.W., 2008. Molecular cytogenetic analysis and resequencing of contactin associated protein-like 2 in autism spectrum disorders. Am. J. Hum. Genet. 82 (1), 165–173.

Boada, L., Lahera, G., Pina-Camacho, L., Merchán-Naranjo, J., Díaz-Caneja, C.M., Bellón, J.M., Ruiz-Vargas, J.M., Parellada, M., 2020. Social Cognition in Autism and Schizophrenia Spectrum Disorders: The Same but Different? J. Autism Dev. Disord. 50 (8), 3046–3059.

Canali G, Garcia M, Hivert B, Pinatel D, Goullancourt A, Oguievetskaia K, et al. Genetic variants in autism-related CNTNAP2 impair axonal growth of cortical neurons. Hum. Mol. Genet. 2018;27:1941-1954.

Caruana, F., Avanzini, P., Gozzo, F., Pelliccia, V., Casaceli, G., Rizzolatti, G., 2016. A Mirror Mechanism for Smiling in the Anterior Cingulate Cortex. Emotion 17 (2), 187–190.

Catani, M., Dell'Acqua, F., Budisavljevic, S., Howells, H., Thiebaut de Schotten, M., Froudist-Walsh, S., D'Anna, L., Thompson, A., Sandrone, S., Bullmore, E.T., Suckling, J., Baron-Cohen, S., Lombardo, M.V., Wheelwright, S.J., Chakrabarti, B., Lai, M.-C., Ruigrok, A.N.V., Leemans, A., Ecker, C., MRC.AIMS. Consortium, Craig, M.C., Murphy, D.G.M., 2016. Frontal networks in adults with autism spectrum disorder. Brain 139 (2), 616–630.

Cauda, F., Geda, E., Sacco, K., D'Agata, F., Duca, S., Geminiani, G., Keller, R., 2011. Grey matter abnormality in autism spectrum disorder: an activation likelihood estimation meta-analysis study. J. Neurol. Neurosurg. Psychiatry 82 (12), 1304–1313.

Chen, C.-H., Chen, H.-I., Chien, W.-H., Li, L.-H., Wu, Y.-Y., Chiu, Y.-N., Tsai, W.-C., Gau, S.-F., 2017. High resolution analysis of rare copy number variants in patients with autism spectrum disorder from Taiwan. Sci. Rep. 7 (1) https://doi.org/10.1038/s41598-017-12081-4.

Chen, Y.L., Chen, W.J., Lin, K.C., Shen, L.J., Gau, S.S., 2019. Prevalence of DSM-5 mental disorders in a nationally representative sample of children in Taiwan: methodology and main findings. Epidemiol. Psychiatr. Sci. 30, 1–9.

Chiang, H.-L., Chen, Y.-J., Lin, H.-Y., Tseng, W.-Y., Gau, S.-F., 2017. Disorder-Specific Alteration in White Matter Structural Property in Adults With Autism Spectrum Disorder Relative to Adults With ADHD and Adult Controls. Hum. Brain Mapp. 38 (1), 384–395.

Chiang, H.-L., Kao, W.-C., Chou, M.-C., Chou, W.-J., Chiu, Y.-N., Wu, Y.-Y., Gau, S.-F., 2018. School dysfunction in youth with autistic spectrum disorder in Taiwan: The effect of subtype and ADHD. Autism Res. 11 (6), 857–869.

Chien, Y.-L., Tu, E.-N., Gau, S.-F., 2017. School Functions in Unaffected Siblings of Youths with Autism Spectrum Disorders. J. Autism Dev. Disord. 47 (10), 3059–3071.

Clemm von Hohenberg, C., Wigand, M.C., Kubicki, M., Leicht, G., Giegling, I., Karch, S., et al., 2013. CNTNAP2 polymorphisms and structural brain connectivity: a diffusion-tensor imaging study. J. Psychiatr. Res. 47, 1349–1356.

Constantino, J.N., Gruber, C.P., 2005. Social Responsiveness Scale (SRS) manual. Western Psychological Services, Los Angeles, CA, USA.

Dale, A.M., Fischl, B., Sereno, M.I., 1999. Cortical surface-based analysis. I. Segmentation and surface reconstruction. Neuroimage 9 (2), 179–194.

Dennis, E.L., Jahanshad, N., Rudie, J.D., Brown, J.A., Johnson, K., McMahon, K.L., de Zubicaray, G.I., Montgomery, G., Martin, N.G., Wright, M.J., Bookheimer, S.Y., Dapretto, M., Toga, A.W., Thompson, P.M., 2011. Altered structural brain connectivity in healthy carriers of the autism risk gene, CNTNAP2. Brain Connect. 1 (6), 447–459.

Desikan, R.S., Ségonne, F., Fischl, B., Quinn, B.T., Dickerson, B.C., Blacker, D., Buckner, R.L., Dale, A.M., Maguire, R.P., Hyman, B.T., Albert, M.S., Killiany, R.J., 2006. An automated labeling system for subdividing the human cerebral cortex on MRI scans into gyral based regions of interest. Neuroimage 31 (3), 968–980.

Dichter, G.S., Felder, J.N., Bodfish, J.W., 2009. Autism is characterized by dorsal anterior cingulate hyperactivation during social target detection. Soc. Cogn. Affect Neurosci. 4 (3), 215–226.

Doyle-Thomas, K.A.R., Duerden, E.G., Taylor, M.J., Lerch, J.P., Soorya, L.V., Wang, A.T., Fan, J., Hollander, E., Anagnostou, E., 2013. Effects of age and symptomatology on cortical thickness in autism spectrum disorders. Res. Autism Spectr. Disord. 7 (1), 141–150.

Fischl, B., 2012. FreeSurfer. Neuroimage 62 (2), 774–781.

Fischl, B., Dale, A.M., 2000. Measuring the thickness of the human cerebral cortex from magnetic resonance images. Proc. Natl. Acad. Sci. USA 97 (20), 11050–11055.

Fischl, B., Salat, D.H., Busa, E., Albert, M., Dieterich, M., Haselgrove, C., van der Kouwe, A., Killiany, R., Kennedy, D., Klaveness, S., Montillo, A., Makris, N., Rosen, B., Dale, A.M., 2002. Whole brain segmentation: automated labeling of neuroanatomical structures in the human brain. Neuron 33 (3), 341–355.

Fischl, B., Salat, D.H., van der Kouwe, A.J.W., Makris, N., Ségonne, F., Quinn, B.T., Dale, A.M., 2004a. Sequence-independent segmentation of magnetic resonance images. Neuroimage 23, S69–S84.

Fischl, B., van der Kouwe, A., Destrieux, C., Halgren, E., Segonne, F., Salat, D.H., et al., 2004b. Automatically parcellating the human cerebral cortex. Cereb. Cortex 14, 11–22.

Gau, S.S.F., Chong, M.Y., Chen, T.H.H., Cheng, A.T.A., 2005. A 3-year panel study of mental disorders among adolescents in Taiwan. Am. J. Psychiatry 162 (7), 1344–1350.
Gau, S.-F., Ni, H.-C., Shang, C.-Y., Soong, W.-T., Wu, Y.-Y., Lin, L.-Y., Chiu, Y.-N., 2010. Psychiatric comorbidity among children and adolescents with and without persistent attention-deficit hyperactivity disorder. Aust. N. Z. J. Psychiatry 44 (2), 135–143.
Gau, S.-F., Lee, C.-M., Lai, M.-C., Chiu, Y.-N., Huang, Y.-F., Kao, J.-D., Wu, Y.-Y., 2011. Psychometric properties of the chinese version of the social communication questionnaire. Res. Autism Spectr. Disord. 5 (2), 809–818.
Gau, S.-F., Liu, L.-T., Wu, Y.-Y., Chiu, Y.-N., Tsai, W.-C., 2013. Psychometric properties of the Chinese version of the social responsiveness scale. Res Autism Spectr Disord 7 (2), 349–360.
Greimel, E., Nehrkorn, B., Schulte-Rüther, M., Fink, G.R., Nickl-Jockschat, T., Herpertz-Dahlmann, B., Konrad, K., Eickhoff, S.B., 2013. Changes in grey matter development in autism spectrum disorder. Brain Struct. Funct. 218 (4), 929–942.
Han, X., Jovicich, J., Salat, D., van der Kouwe, A., Quinn, B., Czanner, S., Busa, E., Pacheco, J., Albert, M., Killiany, R., Maguire, P., Rosas, D., Makris, N., Dale, A., Dickerson, B., Fischl, B., 2006. Reliability of MRI-derived measurements of human cerebral cortical thickness: the effects of field strength, scanner upgrade and manufacturer. Neuroimage 32 (1), 180–194.
Hau, J., Aljawad, S., Baggett, N., Fishman, I., Carper, R.A., Müller, R.-A., 2019. The cingulum and cingulate U-fibers in children and adolescents with autism spectrum disorders. Hum. Brain Mapp. 40 (11), 3153–3164.
Hsiao, M.-N., Tseng, W.-L., Huang, H.-Y., Gau, S.-F., 2013. Effects of autistic traits on social and school adjustment in children and adolescents: the moderating roles of age and gender. Res. Dev. Disabil. 34 (1), 254–265.
Hyde, K.L., Samson, F., Evans, A.C., Mottron, L., 2010. Neuroanatomical differences in brain areas implicated in perceptual and other core features of autism revealed by cortical thickness analysis and voxel-based morphometry. Hum. Brain Mapp. 31, 556–566.
Jha, S.C., Xia, K., Schmitt, J.E., Ahn, M., Girault, J.B., Murphy, V.A., Li, G., Wang, L.i., Shen, D., Zou, F., Zhu, H., Styner, M., Knickmeyer, R.C., Gilmore, J.H., 2018. Genetic influences on neonatal cortical thickness and surface area. Hum. Brain Mapp. 39 (12), 4998–5013.
Jiao, Y., Chen, R., Ke, X., Chu, K., Lu, Z., Herskovits, E.H., 2010. Predictive models of autism spectrum disorder based on brain regional cortical thickness. Neuroimage 50 (2), 589–599.
Laidi, C., Boisgontier, J., de Pierrefeu, A., Duchesnay, E., Hotier, S., d'Albis, M.-A., Delorme, R., Bolognani, F., Czech, C., Bouquet, C., Amestoy, A., Petit, J., Holiga, Š., Dukart, J., Gaman, A., Toledano, E., Ly-Le Moal, M., Scheid, I., Leboyer, M., Houenou, J., 2019. Decreased cortical thickness in the anterior cingulate cortex in adults with autism. J. Autism Dev. Disord. 49 (4), 1402–1409.
Lau, W.-P., Gau, S.-F., Chiu, Y.-N., Wu, Y.-Y., 2014. Autistic traits in couple dyads as a predictor of anxiety spectrum symptoms. J. Autism Dev. Disord. 44 (11), 2949–2963. https://doi.org/10.1007/s10803-014-2151-5.
Lau, W.K.W., Leung, M.-K., Zhang, R., 2020. Hypofunctional connectivity between the posterior cingulate cortex and ventromedial prefrontal cortex in autism: Evidence from coordinate-based imaging meta-analysis. Prog. Neuro-Psychopharmacol. Biol. Psychiatry 103, 109986. https://doi.org/10.1016/j.pnpbp.2020.109986.
Leech, R., Sharp, D.J., 2014. The role of the posterior cingulate cortex in cognition and disease. Brain 137, 12–32.
Li, X., Hu, Z., He, Y., Xiong, Z., Long, Z., Peng, Y., et al., 2010. Association analysis of CNTNAP2 polymorphisms with autism in the Chinese Han population. Psychiatr. Genet. 20, 113–117.
Libero, L.E., DeRamus, T.P., Lahti, A.C., Deshpande, G., Kana, R.K., 2015. Multimodal neuroimaging based classification of autism spectrum disorder using anatomical, neurochemical, and white matter correlates. Cortex 66, 46–59.
Lo, Y.C., Chen, Y.J., Hsu, Y.C., Chien, Y.L., Gau, S.S., Tseng, W.I., 2019. Altered frontal aslant tracts as a heritable neural basis of social communication deficits in autism spectrum disorder: A sibling study using tract-based automatic analysis. Autism Res. 12, 225–238. https://doi.org/10.1002/aur.2044. Epub 18 Dec 12.
Lord, C., Rutter, M., Le Couteur, A., 1994. Autism Diagnostic Interview-Revised: a revised version of a diagnostic interview for caregivers of individuals with possible pervasive developmental disorders. J. Autism Dev. Disord. 24 (5), 659–685.
Mitelman, S.A., Bralet, M.-C., Haznedar, M.M., Hollander, E., Shihabuddin, L., Hazlett, E. A., Buchsbaum, M.S., 2017. Diametrical relationship between gray and white matter volumes in autism spectrum disorder and schizophrenia. Brain Imaging Behav. 11 (6), 1823–1835.
Murdoch, J.D., Gupta, A.R., Sanders, S.J., Walker, M.F., Keaney, J., Fernandez, T.V., Murtha, M.T., Anyanwu, S., Ober, G.T., Raubeson, M.J., DiLullo, N.M., Villa, N., Waqar, Z., Sullivan, C., Gonzalez, L., Willsey, A.J., Choe, S.-Y., Neale, B.M., Daly, M. J., State, M.W., Flint, J., 2015. No evidence for association of autism with rare heterozygous point mutations in Contactin-Associated Protein-Like 2 (CNTNAP2), or in Other Contactin-Associated Proteins or Contactins. PLoS Genet. 11 (1), e1004852.
Newbury, D.F., Paracchini, S., Scerri, T.S., Winchester, L., Addis, L., Richardson, A.J., Walter, J., Stein, J.F., Talcott, J.B., Monaco, A.P., 2011. Investigation of dyslexia and SLI risk variants in reading- and language-impaired subjects. Behav. Genet. 41 (1), 90–104.
Ni HC, Lin HY, Tseng WI, Chiu YN, Wu YY, Tsai WC, et al. Neural correlates of impaired self-regulation in male youths with autism spectrum disorder: A voxel-based morphometry study. Prog Neuropsychopharmacol Biol. Psychiatry 2018;82:233-241.:10.1016/j.pnpbp.2017.11.008. Epub Nov 9.
Nickl-Jockschat, T., Habel, U., Maria Michel, T., Manning, J., Laird, A.R., Fox, P.T., Schneider, F., Eickhoff, S.B., 2012. Brain structure anomalies in autism spectrum disorder–a meta-analysis of VBM studies using anatomic likelihood estimation. Hum. Brain Mapp. 33 (6), 1470–1489.
O'Roak, B.J., Deriziotis, P., Lee, C., Vives, L., Schwartz, J.J., Girirajan, S., Karakoc, E., MacKenzie, A.P., Ng, S.B., Baker, C., Rieder, M.J., Nickerson, D.A., Bernier, R., Fisher, S.E., Shendure, J., Eichler, E.E., 2011. Exome sequencing in sporadic autism spectrum disorders identifies severe de novo mutations. Nat. Genet. 43 (6), 585–589.
Palomero-Gallagher, N., Mohlberg, H., Zilles, K., Vogt, B., 2008. Cytology and receptor architecture of human anterior cingulate cortex. J. Comp. Neurol. 508 (6), 906–926.
Patriquin, M.A., DeRamus, T., Libero, L.E., Laird, A., Kana, R.K., 2016. Neuroanatomical and neurofunctional markers of social cognition in autism spectrum disorder. Hum. Brain Mapp. 37 (11), 3957–3978.
Peñagarikano, O., Abrahams, B., Herman, E., Winden, K., Gdalyahu, A., Dong, H., Sonnenblick, L., Gruver, R., Almajano, J., Bragin, A., Golshani, P., Trachtenberg, J., Peles, E., Geschwind, D., 2011. Absence of CNTNAP2 leads to epilepsy, neuronal migration abnormalities, and core autism-related deficits. Cell 147 (1), 235–246.
Penagarikano, O., Lazaro, M.T., Lu, X.H., Gordon, A., Dong, H., Lam, H.A., et al., 2015. Exogenous and evoked oxytocin restores social behavior in the Cntnap2 mouse model of autism. Sci. Transl. Med. 7, 271ra8.
Peter, B., Raskind, W.H., Matsushita, M., Lisowski, M., Vu, T., Berninger, V.W., Wijsman, E.M., Brkanac, Z., 2011. Replication of CNTNAP2 association with nonword repetition and support for FOXP2 association with timed reading and motor activities in a dyslexia family sample. J. Neurodev. Disord. 3 (1), 39–49.
Pfefferbaum, A., Sullivan, E.V., Carmelli, D., 2001. Genetic regulation of regional microstructure of the corpus callosum in late life. NeuroReport 12 (8), 1677–1681.
Poliak, S., Salomon, D., Elhanany, H., Sabanay, H., Kiernan, B., Pevny, L., et al., 2003. Juxtaparanodal clustering of Shaker-like K+ channels in myelinated axons depends on Caspr2 and TAG-1. J. Cell Biol. 162, 1149–1160.
Poliak, S., Gollan, L., Martinez, R., Custer, A., Einheber, S., Salzer, J.L., Trimmer, J.S., Shrager, P., Peles, E., 1999. Caspr2, a new member of the neurexin superfamily, is localized at the juxtaparanodes of myelinated axons and associates with K+ channels. Neuron 24 (4), 1037–1047.
Postema, M.C., van Rooij, D., Anagnostou, E., Arango, C., Auzias, G., Behrmann, M., Filho, G.B., Calderoni, S., Calvo, R., Daly, E., Deruelle, C., Di Martino, A., Dinstein, I., Duran, F.L.S., Durston, S., Ecker, C., Ehrlich, S., Fair, D., Fedor, J., Feng, X., Fitzgerald, J., Floris, D.L., Freitag, C.M., Gallagher, L., Glahn, D.C., Gori, I., Haar, S., Hoekstra, L., Jahanshad, N., Jalbrzikowski, M., Janssen, J., King, J.A., Kong, X.Z., Lazaro, L., Lerch, J.P., Luna, B., Martinho, M.M., McGrath, J., Medland, S.E., Muratori, F., Murphy, C.M., Murphy, D.G.M., O'Hearn, K., Oranje, B., Parellada, M., Puig, O., Retico, A., Rosa, P., Rubia, K., Shook, D., Taylor, M.J., Tosetti, M., Wallace, G.L., Zhou, F., Thompson, P.M., Fisher, S.E., Buitelaar, J.K., Francks, C., 2019. Altered structural brain asymmetry in autism spectrum disorder in a study of 54 datasets. Nat. Commun. 10 (1) https://doi.org/10.1038/s41467-019-13005-8.
Posthuma, D., de Geus, E.J., Neale, M.C., Hulshoff Pol, H.E., Baare, W.E.C., Kahn, R.S., et al., 2000. Multivariate genetic analysis of brain structure in an extended twin design. Behav. Genet. 30, 311–319.
Reiner, O., Karzbrun, E., Kshirsagar, A., Kaibuchi, K., 2016. Regulation of neuronal migration, an emerging topic in autism spectrum disorders. J. Neurochem. 136 (3), 440–456.
Rodenas-Cuadrado, P., Ho, J., Vernes, S.C., 2014. Shining a light on CNTNAP2: complex functions to complex disorders. Eur. J. Hum. Genet. 22 (2), 171–178.
Rosen, A.F.G., Roalf, D.R., Ruparel, K., Blake, J., Seelaus, K., Villa, L.P., Ciric, R., Cook, P. A., Davatzikos, C., Elliott, M.A., Garcia de La Garza, A., Gennatas, E.D., Quarmley, M., Schmitt, J.E., Shinohara, R.T., Tisdall, M.D., Craddock, R.C., Gur, R. E., Gur, R.C., Satterthwaite, T.D., 2018. Quantitative assessment of structural image quality. Neuroimage 169, 407–418.
Schmitt, J.E., Lenroot, R.K., Wallace, G.L., Ordaz, S., Taylor, K.N., Kabani, N., et al., 2008. Identification of genetically mediated cortical networks: a multivariate study of pediatric twins and siblings. Cereb. Cortex 18, 1737–1747.
Scott, K.E., Kazazian, K., Mann, R.S., Möhrle, D., Schormans, A.L., Schmid, S., Allman, B. L., 2020. Loss of Cntnap2 in the rat causes autism-related alterations in social interactions, stereotypic behavior, and sensory processing. Autism Res. 13 (10), 1698–1717.
Scott-Van Zeeland, A.A., Abrahams, B.S., Alvarez-Retuerto, A.I., Sonnenblick, L.I., Rudie, J.D., Ghahremani, D., et al., 2010. Altered functional connectivity in frontal lobe circuits is associated with variation in the autism risk gene CNTNAP2. Sci. Transl. Med. 2, 56ra80.
Ségonne, F., Dale, A.M., Busa, E., Glessner, M., Salat, D., Hahn, H.K., Fischl, B., 2004. A hybrid approach to the skull stripping problem in MRI. Neuroimage 22 (3), 1060–1075.
Segonne, F., Pacheco, J., Fischl, B., 2007. Geometrically accurate topology-correction of cortical surfaces using nonseparating loops. IEEE Trans. Med. Imaging 26 (4), 518–529.
Simms, M.L., Kemper, T.L., Timbie, C.M., Bauman, M.L., Blatt, G.J., 2009. The anterior cingulate cortex in autism: heterogeneity of qualitative and quantitative cytoarchitectonic features suggests possible subgroups. Acta Neuropathol. 118 (5), 673–684.
Sled, J.G., Zijdenbos, A.P., Evans, A.C., 1998. A nonparametric method for automatic correction of intensity nonuniformity in MRI data. IEEE Trans. Med. Imaging 17 (1), 87–97.
Strauss, K.A., Puffenberger, E.G., Huentelman, M.J., Gottlieb, S., Dobrin, S.E., Parod, J. M., Stephan, D.A., Morton, D.H., 2006. Recessive symptomatic focal epilepsy and mutant contactin-associated protein-like 2. N. Engl. J. Med. 354 (13), 1370–1377.
Tan, G.C.Y., Doke, T.F., Ashburner, J., Wood, N.W., Frackowiak, R.S.J., 2010. Normal variation in fronto-occipital circuitry and cerebellar structure with an autism-associated polymorphism of CNTNAP2. Neuroimage 53 (3), 1030–1042.
Thompson, P.M., Mega, M.S., Vidal, C., Rapoport, J.L., Toga, A.W., 2001. Detecting disease-specific patterns of brain structure using cortical pattern matching and a

population-based probabilistic brain atlas. Information Processing in Medical imaging: Proceedings of the Conference 2082, 488–501.
Toal, F., Bloemen, O.J.N., Deeley, Q., Tunstall, N., Daly, E.M., Page, L., Brammer, M.J., Murphy, K.C., Murphy, D.G.M., 2009. Psychosis and autism: magnetic resonance imaging study of brain anatomy. Br. J. Psychiatry 194 (5), 418–425.
Toma, C., Hervas, A., Torrico, B., Balmana, N., Salgado, M., Maristany, M., et al., 2013. Analysis of two language-related genes in autism: a case-control association study of FOXP2 and CNTNAP2. Psychiatr. Genet. 23, 82–85.
Toma, C., Pierce, K.D., Shaw, A.D., Heath, A., Mitchell, P.B., Schofield, P.R., et al., 2018. Comprehensive cross-disorder analyses of CNTNAP2 suggest it is unlikely to be a primary risk gene for psychiatric disorders. PLoS Genet. 14.
Tu, P.-C., Hsu, J.-W., Lan, C.-C., Liu, C.-C., Su, T.-P., Chen, Y.-S., 2016. Structural and functional correlates of a quantitative autistic trait measured using the social responsive scale in neurotypical male adolescents. Autism Res. 9 (5), 570–578.
Uddén, J., Snijders, T.M., Fisher, S.E., Hagoort, P., 2017. A common variant of the CNTNAP2 gene is associated with structural variation in the left superior occipital gyrus. Brain Lang. 172, 16–21.
van Rooij, D., Anagnostou, E., Arango, C., Auzias, G., Behrmann, M., Busatto, G.F., Calderoni, S., Daly, E., Deruelle, C., Di Martino, A., Dinstein, I., Duran, F.L.S., Durston, S., Ecker, C., Fair, D., Fedor, J., Fitzgerald, J., Freitag, C.M., Gallagher, L., Gori, I., Haar, S., Hoekstra, L., Jahanshad, N., Jalbrzikowski, M., Janssen, J., Lerch, J., Luna, B., Martinho, M.M., McGrath, J., Muratori, F., Murphy, C.M., Murphy, D.G.M., O'Hearn, K., Oranje, B., Parellada, M., Retico, A., Rosa, P., Rubia, K., Shook, D., Taylor, M., Thompson, P.M., Tosetti, M., Wallace, G.L., Zhou, F., Buitelaar, J.K., 2018. Cortical and subcortical brain morphometry differences between patients with autism spectrum disorder and healthy individuals across the lifespan: results from the ENIGMA ASD Working Group. Am. J. Psychiatry 175 (4), 359–369.
Vernes, S.C., Newbury, D.F., Abrahams, B.S., Winchester, L., Nicod, J., Groszer, M., Alarcón, M., Oliver, P.L., Davies, K.E., Geschwind, D.H., Monaco, A.P., Fisher, S.E., 2008. A functional genetic link between distinct developmental language disorders. N. Engl. J. Med. 359 (22), 2337–2345.
Via, E., Radua, J., Cardoner, N., Happé, F., Mataix-Cols, D., 2011. Meta-analysis of gray matter abnormalities in autism spectrum disorder: should Asperger disorder be subsumed under a broader umbrella of autistic spectrum disorder? Arch. Gen. Psychiatry 68 (4), 409. https://doi.org/10.1001/archgenpsychiatry.2011.27.
Whalley, H.C., O'Connell, G., Sussmann, J.E., Peel, A., Stanfield, A.C., Hayiou-Thomas, M.E., Johnstone, E.C., Lawrie, S.M., McIntosh, A.M., Hall, J., 2011. Genetic variation in CNTNAP2 alters brain function during linguistic processing in healthy individuals. Am. J. Med. Genet. B Neuropsychiatr. Genet. 156 (8), 941–948.
Whitehouse, A.J., Bishop, D.V., Ang, Q.W., Pennell, C.E., Fisher, S.E., 2011. CNTNAP2 variants affect early language development in the general population. Genes Brain Behav. 10, 451–456.
Xiao, Z., Qiu, T., Ke, X., Xiao, X., Xiao, T., Liang, F., et al., 2014. Autism spectrum disorder as early neurodevelopmental disorder: evidence from the brain imaging abnormalities in 2–3 years old toddlers. J. Autism Dev. Disord. 44, 1633–1640.
Yang, X., Si, T., Gong, Q., Qiu, L., Jia, Z., Zhou, M.i., Zhao, Y., Hu, X., Wu, M., Zhu, H., 2016. Brain gray matter alterations and associated demographic profiles in adults with autism spectrum disorder: A meta-analysis of voxel-based morphometry studies. Aust. N. Z. J. Psychiatry 50 (8), 741–753.
Yin, C.-L., Chen, H.-I., Li, L.-H., Chien, Y.-L., Liao, H.-M., Chou, M.C., Chou, W.-J., Tsai, W.-C., Chiu, Y.-N., Wu, Y.-Y., Lo, C.-Z., Wu, J.-Y., Chen, Y.-T., Gau, S.-F., 2016. Genome-wide analysis of copy number variations identifies PARK2 as a candidate gene for autism spectrum disorder. Mol. Autism. 7 (1) https://doi.org/10.1186/s13229-016-0087-7.
Zhang, T., Zhang, J., Wang, Z., Jia, M., Lu, T., Wang, H., Yue, W., Zhang, D., Li, J., Wang, L., 2019. Association between CNTNAP2 polymorphisms and autism: A family-based study in the chinese han population and a meta-analysis combined with GWAS data of psychiatric genomics consortium. Autism. Res. 12 (4), 553–561.
Zhu, B.i., Chen, C., Xue, G., Lei, X., Wang, Y., Li, J., Moyzis, R.K., Li, J., Dong, Q.i., Lin, C., 2017. Associations between the CNTNAP2 gene, dorsolateral prefrontal cortex, and cognitive performance on the Stroop task. Neuroscience 343, 21–29.
Zikopoulos, B., Barbas, H., 2010. Changes in prefrontal axons may disrupt the network in autism. J. Neurosci. 30 (44), 14595–14609.
Zikopoulos, B., García-Cabezas, M.Á., Barbas, H., Darian-Smith, C., 2018. Parallel trends in cortical gray and white matter architecture and connections in primates allow fine study of pathways in humans and reveal network disruptions in autism. PLoS Biol. 16 (2), e2004559.